Applicable Analysis and Discrete Mathematics
available online at http://pefmath.etf.rs

Appl. Anal. Discrete Math. **8** (2014), 33–59. doi:10.2298/AADM140126002M

EFFECTIVE ROUGH BOUNDARY PARAMETRIZATION FOR REACTION-DIFFUSION SYSTEMS

C. Mocenni, E. Sparacino, J. P. Zubelli

We address the problem of parametrizing the boundary data for reaction-diffusion partial differential equations associated to distributed systems that possess rough boundaries. The boundaries are modeled as fast oscillating periodic structures and are endowed with Neumann or Dirichlet boundary conditions. Using techniques from homogenization theory and multiple-scale analysis we derive the effective equation and boundary conditions that are satisfied by the homogenized solution. We present numerical simulations that validate our theoretical results and compare it with the alternative approach based on solving the same equation with a smoothed version of the boundary. The numerical tests show the accuracy of the homogenized solution to the effective system vis a vis the numerical solution of the original differential equation. The homogenized solution is shown undergoing dynamical regime shifts, such as anticipation of pattern formation, obtained by varying the diffusion coefficient.

1. INTRODUCTION AND MOTIVATION

A large variety of natural systems can be modeled by parabolic partial differential equations. Examples of such systems include physical, physiological, ecological and social phenomena displaying complex spatio-temporal dynamics. An important class of such equations is represented by reaction-diffusion equations (see for example [**26**] and references therein). However, the domain where such systems evolve may show complex geometric features, such as porous media and rough boundaries. This fact leads to serious practical as well as theoretical challenges. For example, many sophisticated PDE solvers balk in handling the fine

2010 Mathematics Subject Classification. 35B27, 35Q80, 35K57.
Keywords and Phrases. Reaction-diffusion equations, multiple-scale analysis, rough boundaries.

scales of the boundary. Furthermore, the roughness of the boundary may induce noise and uncertainty in measuring the state variables of the system close to the boundary. These factors lead to many difficulties in the approximation and identification of the mathematical models describing the actual physical system. Indeed, the approximation of physical systems in the presence of multiple scales requires substantial additional numerical precision and more sophisticated solvers, whereas the identification of the model may fail due to lack of measurements.

One possible approach to these problems consists in generating an equivalent system, defined on a smoothed layer containing the domain, whose parameters near the boundary depend on the rough geometry and such that the solution in the interior of the spatial domain is very close to the one of the original system. As verified in our simulations and intuitively natural, we expect this approach to be preferable than applying simple smoothing or chopping techniques to the boundary.

To this aim, a natural idea would be to gather the leading contribution of such rough domains by some kind of multiple scale analysis. The usual approach for analyzing rough boundaries is the homogenization method (see for example [**30, 18, 17, 45**]). Many other physical systems have been analyzed in the context of complex morphology of domains (see, for example, [**44, 24**] for the case of nonlinear waves over highly variable domains). However, to the authors' knowledge, very little has been done in the specific case of a rough boundary analysis of reaction-diffusion equations.

Once the problem of the numerical convergence of the solutions is addressed, the influence of the roughness on the spatio-temporal dynamics of the system can be more easily investigated. In fact, the presence of complex boundaries may produce important modifications in the asymptotic distribution of the model variables.

For example, in the field of ecological modeling, it is well known from the literature, that lakes with complex geometry show larger spatial variability of limnological parameters than lakes with a simple shape. In [**31**] it is shown, for example, that the Pilkington Bay, a shallow, eutrophic embayment with a complex geometry in northwestern Lake Victoria, East Africa is strongly influenced by differences in rates of heating, cooling, and depth of wind mixing with respect to a lake with a simple shape. Regarding the ecological processes in lakes with rough boundaries, Assireu et al. [**12**] have observed that correlations between geometrical complexity and phytoplankton distribution are present in some Amazonian lakes. The authors are involved in projects aimed at modeling the amazon lake of Serra da Mesa [**41**] in a distributed system set up. However, the roughness of the boundary conditions required the development of novel techniques to parametrize effectively the boundary.

In this work, homogenization is used to analyze a class of reaction diffusion equations in domains with rough boundaries. In particular, it is shown that such boundary can be replaced by an equivalent layer where a modified differential equation holds. The coefficients in this new equation are certain effective parameters, such as the effective diffusivity, determined by solving a homogenized problem involving the geometry of the boundary. After the formal asymptotic expansion is

developed, it will be validated through numerical experiments. Convergence of the homogenized solution is then verified by numerical simulations. The effects of the rough boundaries in the dynamics are quantified by comparing the homogenized system and a system with the same mathematical structure simulated in a regular domain. In particular, two systems showing complex spatio-temporal patterns are analyzed and the quantification of the changes in their dynamical properties are measured by using a suitable recurrence indicator.

The paper is organized as follow: In Section 2 we describe the class of reaction diffusion models that will be analyzed and the formal asymptotic expansion. In Section 3 we perform the homogenization and provide the equation satisfied by the leading term of the formal asymptotic expansion. This section follows very closely the work of Nevard and Keller [**45**], with main differences concerning the fact that our system is nonlinear and time dependent. In Section 4 we present the numerical simulations to validate the asymptotic expansion. After the comparison of the homogenized systems with a smoothed one, developed in Section 4 and the application to a multispecies ecological model, described in Section 5, the effects of rough boundaries in the dynamics of complex systems are investigated in Section 6 by means of recurrence indicators. Conclusion are drawn in Section 7 with some final remarks and directions for future research.

1.1. Literature review

We close the Introduction with a short literature survey of homogenization works in the present context so as to place this article in perspective. Homogenization has been the subject of huge attention during the past few decades. See for example [**21, 20**] and references therein. Although we shall refrain from the temptation of trying to present a comprehensive description of such literature, we will try to cover a few points that seem to be closer to the subject of rough boundary homogenization and the ecological applications we have in mind.

The study of effective conditions in the context of partial differential equations in fluid dynamics has been the subject of extensive studies in the literature. In many contexts such conditions are called *wall laws*. In [**1**] two ways of deriving wall-laws for incompressible viscous flows on rough surface were analyzed. In [**4**] the effective boundary conditions were proposed for a laminar flow over a rough wall with periodic roughness elements. In [**2**] the problem of simulating flows over a rough surface or flows with strong gradients near walls was considered and numerical tests were performed. In [**3**] an error estimate for the approximation of the Dirichlet problem with complex boundaries by wall laws is presented.

More recently a lot of numerical, as well as theoretical, research has been developed in the context of the finite element method for rough boundaries. See for example [**32, 33**] for the case of elliptic equations and [**19**] in the specific case of the heat equation.

In the context of time-independent (elliptic) problems an enthralling survey could be found in [**46**]. Here, the focus is on the interior of the domain, and not on the boundary, although one may certainly conjecture about the extension of such

ideas to rough or random boundary conditions.

The state of the art on the homogenization of rapidly oscillating boundaries is evolving very fast. Indeed, in [**9, 10, 8, 11, 47**] thin domains with highly oscillatory boundaries have been studied in a theoretical framework and convergence results have been obtained, mostly for elliptic or stationary problems. In comparison with our work we do not assume a thin domain.

In [**5**], Amirat et al. study the asymptotic behavior of the solution of the Laplace equation in a domain, whose boundary includes a highly oscillating part. Using a boundary layer corrector, they derive and analyze a non-oscillating approximation of the solution in the H^1 norm. In reference [**6**], the same authors deal with the modeling of a Stokes flow. Here, the domain is bounded above by a periodic distribution of small asperities. An asymptotic expansion is obtained and as the period tends to zero, the solution of the problem converges to its leading term. The asymptotic expansion convergence is justified through error estimates. In [**7**], the authors determine effective boundary conditions and find asymptotic approximations, which can be exploited in numerical schemes. More precisely, they derive a wall law for the flow over a very rough surface according to the steady Stokes equations. The approximation's accuracy is characterized in terms of the small parameter ϵ. The latter measures the size of the base area of the box-shaped features forming the roughness on the surface of the domain.

In contradistinction with most of the works mentioned above, our focus is towards obtaining simple effective boundary conditions in the context of reaction-diffusion equations, to check their validity in numerical simulations, and to apply it to ecological studies. Our interest stems from the importance of the effects caused by the boundaries on the spatial-temporal diversity of the dynamics. This has attracted the attention of biologists and limnologists as in [**14, 49, 38, 50**].

2. THE MODEL

Consider a rectangular domain Ω_ϵ whose boundary is partly rough with periodic roughness elements Γ_ϵ. To model this boundary, we shall use the curve $z = h(x/\epsilon)$ in the (x, z) plane of period ϵ in x. Here ϵ refers to the basic scale where the boundary oscillation takes place and is assumed to be much smaller than the characteristic dimensions of our domain. Following [**45**], we assume that the boundary oscillates between the lines $z = -A$ and $z = 0$. Furthermore, we assume that $z = h(x/\epsilon)$ is monotone in the semi-period and is a differentiable function. Figure 1 shows a schematic representation of the rough periodic boundary, where $\mathbf{n}$ is the outward unit normal vector to the boundary and $\sigma > 0$ represents the diffusivity in the internal domain $z > h(x/\epsilon)$.
We assume that the dynamics of the system is described by the following equation:

$$\frac{\partial U(x,z,t)}{\partial t} - \nabla \cdot (\sigma \nabla U(x,z,t)) = f(U(x,z,t)),\ (x,z) \text{ in } \Omega_\epsilon \ \&\ t \geq 0 \tag{1}$$

subject to appropriate boundary conditions of Dirichlet *or* Neumann type, namely:

$$\text{Neumann:} \qquad \mathbf{n} \cdot (\sigma \nabla U(x,z)) = 0\ ,\ (x,z) \text{ on } \Gamma_\epsilon\ , \tag{2}$$

or

$$\text{Dirichlet:} \qquad U(x,z) = 0 \ , \ (x,z) \text{ on } \Gamma_\epsilon \ , \tag{3}$$

and suitable smooth initial conditions.

We assume that the system under consideration admits solutions in an interval of time independent of ϵ and that the nonlinear function f admits a Taylor expansion at any point.

Our results concern the formal asymptotics in compact subsets of the interior of the homogenized domain and we are not concerned with any possible transient oscillations for arbitrarily small times near the boundary. It is well-known that certain reaction-diffusion systems may not even have solutions for all times. Thus, without further hypothesis on the function f we cannot expect rigorous convergence results. The issue of well-posedness for such systems is the subject of intense research and we shall not dwell on it (see for example [**26**] and references therein).

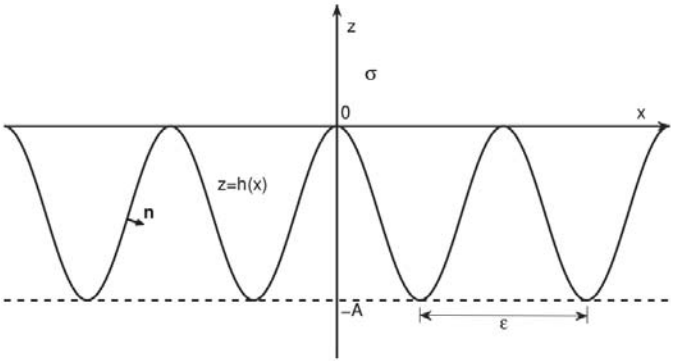

Figure 1. Pictorial description of a boundary segment. The upper part ($z > h(x/\epsilon)$) represents a subset of the internal domain, the periodic curve ($z = h(x)$) is the boundary and the dashed line ($z = -A$) is the external lower boundary.

3. MODEL PARAMETERIZATION USING MULTISCALE ANALYSIS

In this section we present the main results concerning the model parameterization. In particular, two main theorems, accounting for the formal asymptotic analysis of the Neumann and Dirichlet cases, are reported.

Rough boundaries correspond to the intuitive idea of a highly oscillating and unpredictable curve. In other words, the characteristic length of the autocorrelation for the stochastic process that describes the boundary is $\epsilon << 1$ where 1 corresponds to the typical scale of our domain. The stochastic treatment of such problems requires technicalities that would take us to far afield. Instead, we will follow the tradition of homogenization theory [**29**] where weak autocorrelations in random structures are replaced with periodic regions with period $\epsilon \to 0$.

The basic model under consideration is that of equation (1) with boundary conditions given either by equation (3) or by equation (2). We introduce the variable $y = x/\epsilon$ and write U as function of x, y, z, t and ϵ: $U(x, z, t, \epsilon) = u(x, y, z, t, \epsilon)$. Then, we substitute U with u in (1), (3) and (2), noting that $\nabla_x U = (\nabla_x + \epsilon^{-1}\nabla_y)u$ and $\mathbf{n} = [\epsilon^{-1}\nabla_y, -\nabla_z]h$. Thus, we obtain

$$\frac{\partial u}{\partial t} - [\nabla_x + \epsilon^{-1}\nabla_y, \nabla_z]\left(\sigma \begin{bmatrix} \nabla_x + \epsilon^{-1}\nabla_y \\ \nabla_z \end{bmatrix} u\right) - f(u) = 0 \tag{4}$$

and, from (3)

$$\sigma \cdot [\epsilon^{-1}\nabla_y, -\nabla_z]h \cdot \begin{bmatrix} \nabla_x + \epsilon^{-1}\nabla_y \\ \nabla_z \end{bmatrix} u = 0. \tag{5}$$

A straightforward computation using equation (4) yields

$$u_t - \epsilon^{-2}(\sigma u_y)_y - \epsilon^{-1}(\sigma u_x)_y - \epsilon^{-1}(\sigma u_y)_x - (\sigma u_x)_x - (\sigma u_z)_z - f(u) = 0,\ z > h(y), \tag{6}$$

with the following boundary conditions:

$$\sigma(\epsilon^{-2}h_y u_y + \epsilon^{-1}h_y u_x - u_z) = 0, \quad z = h(y), \tag{7}$$

or

$$u = 0, \quad z = h(y)\ . \tag{8}$$

Here, u is required to be periodic in y with period 1, which is the period of the curve $z = h(y)$. See Figure 1. In the sequel, we assume that u can be expanded for ϵ small in the form

$$u(x, y, z, t, \epsilon) = u^{(0)}(x, y, z, t) + \epsilon u^{(1)}(x, y, z, t) + \epsilon^2 u^{(2)}(x, y, z, t) + O(\epsilon^3). \tag{9}$$

and provide the main homogenization results for the Neumann and Dirichlet boundary conditions.

3.1. Neumann boundary conditions

We first consider the case for which, on the rough boundary, we have Neumann boundary conditions described in equation (3).

Following Nevard and Keller [**45**], let us introduce $y_1(z)$ and $y_2(z)$ as two inverses of $z = h(y)$ over one period. The first, $y_1(z)$, increases from $y_1 = 0$ at $z = 0$ to $y_1 = y_1(-A)$ at $z = -A$, and $y_2(z)$ increases from $y_2(-A) = y_1(-A)$ to $y_2(0) = 1$ as z increases from $-A$ to 0 (see Figure 2).

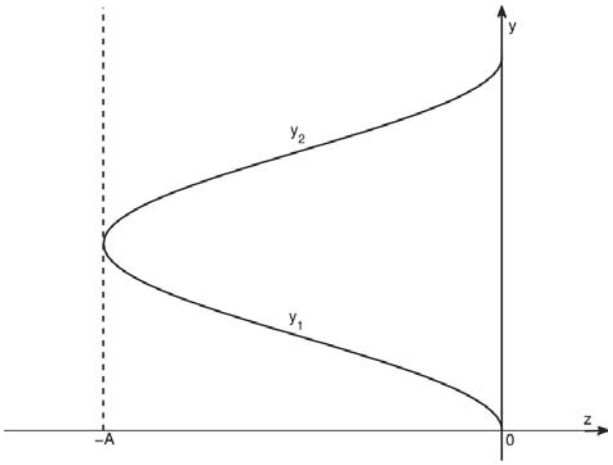

Figure 2. Pictorial description of functions $y_1(z)$ and $y_2(z)$, two inverses of $z = h(y)$.

We can then summarize the main result in the following theorem:

Theorem 1. *Let $U(x, z, t, \epsilon)$ satisfy the reaction-diffusion equation* (1) *with boundary condition* (3) *on $z = h(y)$ a differentiable* 1*-periodic function. Suppose that $U = u(x, y, z, t, \epsilon)$ has the asymptotic form* (9)*, where u is* 1*-periodic in y. Then, $u^{(0)}(x, z, t)$ is independent of y for $-A \le z \le 0$ and is a solution of the problem*:

$$\text{(10a)} \qquad \frac{\partial u^{(0)}}{\partial t} - \nabla \cdot (\sigma \nabla u^{(0)}) - f(u^{(0)}) = 0, \quad z > 0$$

$$\text{(10b)} \qquad \frac{\partial u^{(0)}}{\partial t} - (y_2 - y_1)^{-1} \nabla \cdot (\sigma_{eff} \nabla u^{(0)}) - f(u^{(0)}) = 0, \quad -A < z < 0$$

$$u^{(0)}, \langle\sigma\rangle u_z^{(0)} \qquad \textit{continuous} \quad \textit{at} \quad z = 0$$

$$u_z^{(0)} = 0, \quad z = -A$$

where $\langle\sigma\rangle = \sigma(y_2 - y_1)$ and σ_{eff} is the effective diffusivity tensor:

$$\sigma_{eff} = \begin{pmatrix} 0 & 0 \\ 0 & \langle\sigma\rangle \end{pmatrix}.$$

Proof. First of all, we substitute (9) for u into (6) and (7) obtaining:

$$\text{(11a)} \quad \epsilon^{-2}(-\sigma u_{yy}^{(0)}) + \epsilon^{-1}(-\sigma u_{yy}^{(1)} - \sigma u_{xy}^{(0)} - \sigma u_{yx}^{(0)}) + (u_t^{(0)} - \sigma u_{xy}^{(1)} - \sigma u_{yx}^{(1)} - \sigma u_{xx}^{(0)} - \sigma u_{zz}^{(0)} - f(u^{(0)}) - \sigma u_{yy}^{(2)}) = 0, \quad z > h(y)$$

$$\text{(11b)} \quad \sigma(\epsilon^{-2} h_y u_y^{(0)} + \epsilon^{-1} h_y u_y^{(1)} + h_y u_y^{(2)} + \epsilon^{-1} h_y u_x^{(0)} + h_y u_x^{(1)} - u_z) = 0, \ z = h(y).$$

Then, we equate to zero separately the coefficients of each power of ϵ. For ϵ^{-2} we

obtain

$$\sigma u^{(0)}_{yy} = 0, \quad z > h(y), \tag{12a}$$

$$\sigma u^{(0)}_{y} = 0, \quad z = h(y). \tag{12b}$$

The solution of this problem is the sum of a linear term in y and another one independent of y, namely: $u^{(0)} = \alpha y + \beta$. Furthermore, since u is assumed to be periodic in y, then the linear term in y vanishes. Hence $u^{(0)}$ is independent of y, i.e.,

$$u^{(0)} = u^{(0)}(x, z, t). \tag{13}$$

The coefficient of ϵ^{-1} in (11) yields the following problem for $u^{(1)}$:

$$-\sigma u^{(1)}_{yy} = \sigma u^{(0)}_{xy} + \sigma u^{(0)}_{yx}, \quad z > h(y), \tag{14a}$$

$$\sigma(u^{(1)}_{y} + u^{(0)}_{x}) = 0. \quad z = h(y), \tag{14b}$$

Because $u^{(0)}$ is independent of y, equations (14) become

$$\sigma u^{(1)}_{yy} = 0, \quad z > h(y), \tag{15a}$$

$$\sigma(u^{(1)}_{y} + u^{(0)}_{x}) = 0, \quad z = h(y), \tag{15b}$$

Thus, by integrating (15a) from y_1 to y, with respect to y, and using (15b), we find that:

$$u^{(1)} = (y_1 - y)u^{(0)}_{x}(x, z) + u^{(1)}(x, y_1, z), \quad h(y) \le z \le 0. \tag{16}$$

From the coefficient ϵ^0 we obtain:

$$\sigma u^{(2)}_{yy} + \sigma u^{(1)}_{xy} = -\sigma u^{(1)}_{yx} - \sigma u^{(0)}_{xx} - \sigma u^{(0)}_{zz} + u^{(0)}_{t} - f(u^{(0)}), \quad z > h(y), \tag{17a}$$

$$\sigma(h_y u^{(2)}_{y} + h_y u^{(1)}_{x} - u^{(0)}_{z}) = 0, \quad z = h(y), \tag{17b}$$

Integrating both sides of (17a) between $y_1(z)$ and $y_2(z)$, we get

$$\int_{y_1}^{y_2} \sigma u^{(2)}_{yy} + \sigma u^{(1)}_{xy} = \int_{y_1}^{y_2} -\sigma u^{(1)}_{yx} - \sigma u^{(0)}_{xx} - \sigma u^{(0)}_{zz} + u^{(0)}_{t} - f(u^{(0)}), \tag{18}$$

and from equation (16) we get $u^{(1)}_{y} = -u^{(0)}_{x}$. Hence equation (18) becomes:

$$\begin{aligned} \int_{y_1}^{y_2} \sigma u^{(2)}_{yy} + \sigma u^{(1)}_{xy} &= \int_{y_1}^{y_2} -\sigma u^{(0)}_{zz} + u^{(0)}_{t} - f(u^{(0)}) \\ &= -\langle\sigma\rangle u^{(0)}_{zz} + (y_2 - y_1)(u^{(0)}_{t} - f(u^{(0)})), \end{aligned} \tag{19}$$

where $\langle\sigma\rangle = \sigma(y_2 - y_1)$. Now, on the left hand side of (19) we have

$$\int_{y_1}^{y_2} \sigma u^{(2)}_{yy} + \sigma u^{(1)}_{xy} = (\sigma u^{(2)}_{y} + \sigma u^{(1)}_{x})\Big|_{y_1}^{y_2}, \tag{20}$$

and from (17b) we obtain

$$(\sigma u_y^{(2)} + \sigma u_x^{(1)}) = \sigma \frac{u_z^{(0)}}{h_y} \ .$$

Thus, (20) becomes

$$\int_{y_1}^{y_2} \sigma u_{yy}^{(2)} + \sigma u_{xy}^{(1)} = \sigma \left(\frac{1}{h_y(y_2)} - \frac{1}{h_y(y_1)} \right) u_z^{(0)} \tag{21}$$

Since

$$\frac{\mathrm{d}y_i}{\mathrm{d}z} = \frac{1}{h_y(y_i)}, i = 1, 2 \ ,$$

the right hand side of (21) is

$$\int_{y_1}^{y_2} \sigma u_{yy}^{(2)} + \sigma u_{xy}^{(1)} = \sigma \left(\frac{1}{h_y(y_2)} - \frac{1}{h_y(y_1)} \right) u_z^{(0)} = \langle \sigma \rangle_z u_z^{(0)}. \tag{22}$$

Using this remark on the left hand side of (19) we get

$$(y_2 - y_1) u_t^{(0)} - \sigma((y_2 - y_1) u_z^{(0)})_z - (y_2 - y_1) f(u^{(0)}) = 0, \quad -A < z < 0 \ . \tag{23}$$

This is the equation for $u^{(0)}$ which holds in the interval $-A < z < 0$, within which the boundary oscillates (equation (10b)). We note that the flux continuity condition at $z = 0$ is just the continuity of $u_z^{(0)}$ there. Moreover, regularity of the solution requires that $u_z^{(0)} = 0$ at $z = -A$.

3.2. Dirichlet boundary conditions

We consider now, the case for which, on the rough boundary, we have Dirichlet boundary conditions accounted by equation (2). Assuming, once again, that u can be expanded for ϵ small in the form (9), we can summarize the main result in the following theorem:

Theorem 2. *Let $U(x, z, t, \epsilon)$ satisfy the reaction-diffusion equation (1) with Dirichlet boundary condition (2) on $z = h(y)$, where $h(y)$ is a 1-periodic differentiable function in y. Suppose that $U = u(x, y, z, t, \epsilon)$ has the asymptotic form (9), where u is 1-periodic in y. Then, $u^{(0)}(x, z, t)$ is independent of y for $-A \leq z \leq 0$ and is a solution of the problem:*

$$\frac{\partial u^{(0)}}{\partial t} - \nabla \cdot (\sigma \nabla u^{(0)}) - f(u^{(0)}) = 0, \quad z > 0 \tag{24a}$$

$$u^{(0)} = 0, \quad -A \leq z \leq 0 \tag{24b}$$

Proof. We substitute the expansion in (9) for u into (6) and (8):

$$\begin{aligned}(25a)\quad & \epsilon^{-2}(-\sigma u^{(0)}_{yy}) + \\ & \epsilon^{-1}(-\sigma u^{(1)}_{yy} - \sigma u^{(0)}_{xy} - \sigma u^{(0)}_{yx}) + \\ & (u^{(0)}_t - \sigma u^{(1)}_{xy} - \sigma u^{(1)}_{yx} - \sigma u^{(0)}_{xx} - \sigma u^{(0)}_{zz} - f(u^{(0)}) - \sigma u^{(2)}_{yy}) = 0, \quad z > h(y) \\ (25b)\quad & u^{(0)} = 0, \quad z = h(y).\end{aligned}$$

Then, we equate to zero separately the coefficients of each power of ϵ. For ϵ^{-2} we obtain

$$\sigma u^{(0)}_{yy} = 0, \quad z > h(y), \tag{26a}$$

$$u^{(0)} = 0, \quad z = h(y), \tag{26b}$$

The solution of this problem is

$$u^{(0)} = 0, \quad h(y) < z < 0, \tag{27a}$$

$$u^{(0)} = u^{(0)}(x, z), \quad z > 0. \tag{27b}$$

Thus, for the Dirichlet boundary condition (8), the leading term in the solution $u^{(0)}(x, z)$ satisfies (1) for $z > 0$, with $u^{(0)}(x, 0) = 0$, while $u^{(0)} = 0$ in the layer $-A \leq z \leq 0$. In this case, the rough boundary has the same effect as if it were replaced by the line $z = 0$, which is its upper boundary. □

In the next section we use numerical simulations to test convergence of the expansion (9) to the solution according to theorems 1 and 2 as $\epsilon \to 0$. In other words, we will provide numerical evidence that:

$$u_\epsilon \to u^{(0)} \quad \text{as} \quad \epsilon \to 0 \ ,$$

at least for a class of models commonly used in ecological modeling context [**43**]. To this aim, we note that the roughness of the boundary increases as ϵ decreases. Then, we consider several domains with periodic boundaries with different frequencies and compare numerical solutions of equation (1) (or equation (6) where ϵ is introduced) with the homogenized solution obtained by theorems 1 and 2 with Neumann and Dirichlet boundary conditions, respectively.

4. NUMERICAL VALIDATION

In order to numerically validate the results, we apply the method to a non-linear model describing the distribution of a population in a domain with rough periodic boundaries. The discretization is performed by means of a finite element method of lines whose implementation is available in the software package Comsol Multiphysics. Numerical simulations are performed by means of the well-known

Finite Element Method (see [**27**] for details) and the iterative Generalized Minimal Residual Method (GMRES) available in the software package Comsol Multiphysics (see [**15, 16**] for the convergence properties of the Comsol finite element solution).

The model is described by equation (1) where the reaction term $f(U)$ is given by the following nonlinear logistic equation [**43**]:

$$f(U) = rU\left(1 - \frac{U}{k}\right)$$

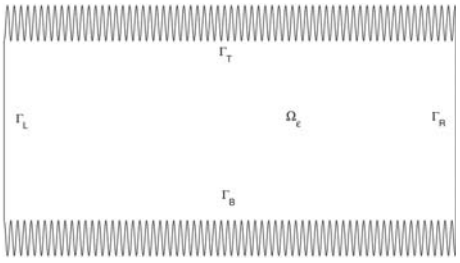

Figure 3. The original domain with a partially rough boundary.

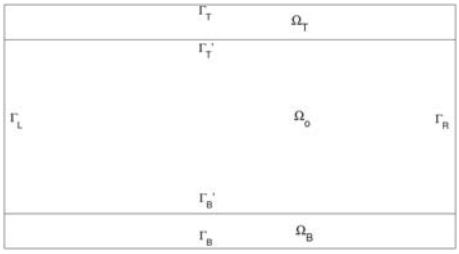

Figure 4. The homogenized domain. $\Omega_h = \Omega_O \cup \Omega_T \cup \Omega_B$.

Let Ω be a rectangular domain whose boundary is defined as $\partial\Omega = \Gamma_L \cup \Gamma_R \cup \Gamma_T \cup \Gamma_B$ (see Figure 3), where Γ_T and Γ_B are highly oscillating periodic functions (with period ϵ in x) described by the following curves:

$$h_T(x/\epsilon) = \frac{A}{2}\cos\left(2\pi\frac{x}{\epsilon}\right) - \frac{A}{2} \text{ and} \tag{28a}$$

$$h_B(x/\epsilon) = -\frac{A}{2}\cos\left(2\pi\frac{x}{\epsilon}\right) - \frac{A}{2} + D\ , \tag{28b}$$

where A is the amplitude of the boundary and D is the vertical displacement between the two rough boundaries. We consider separately the case in which we have Neumann ($\mathbf{n}\cdot(\sigma\nabla U) = 0$) and Dirichlet ($U = 0$) boundary conditions on these two curves, while, on the vertical boundaries Γ_L and Γ_R, we have the following boundary conditions:

Dirichlet	$U = U_L$	on	Γ_L
Neumann	$\mathbf{n}\cdot(\sigma\nabla U) = -k_f U$	on	Γ_R.

Figure 4 describes the homogenized domain $\Omega_h = \Omega_O \cup \Omega_T \cup \Omega_B$, where the rough boundaries, Γ_T and Γ_B in the original domain, are replaced with two equivalent layers where two modified differential equations hold. The coefficients of these new equations are determined by solving a homogenized problem, as reported in theorems 1 and 2 for Neumann and Dirichlet boundary conditions, respectively. The following subsections report simulation results.

First of all, we notice that the use of homogenization simplifies the computational problem by reducing drastically the number of triangular elements in the homogenized domain up to 5% of those present in the rough one. This result is evident from Figure 5, where an example of the mesh in the two cases is reported.

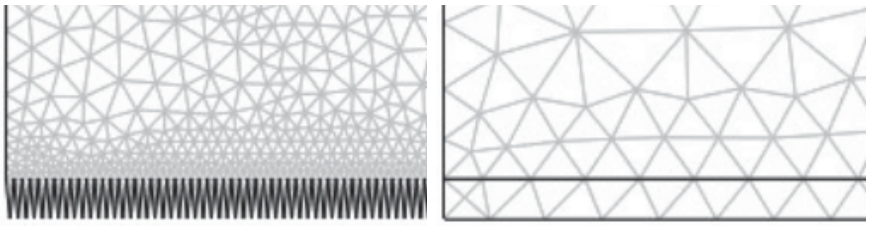

Figure 5. Example of the triangular mesh in the rough (left) and homogenized (right) domains for both Neumann and Dirichlet cases. The total number of elements in this case reduces from 2850 (rough domain) to 140 (homogenized domain).

In order to compare the solutions in the two cases, we start by considering the case for which we have Neumann boundary conditions ($\mathbf{n}\cdot(\sigma\nabla U)$=0) on rough boundaries Γ_T and Γ_B. Theorem (1) leads to the following equations accounting for the Neumann homogenization problem:

$$
\begin{aligned}
&\frac{\partial u^{(0)}}{\partial t} - \nabla\cdot(\sigma\nabla u^{(0)}) = r u^{(0)}\left(1-\frac{u^{(0)}}{k}\right), \quad \text{in} \quad \Omega_O\\
&\frac{\partial u^{(0)}}{\partial t} - (\psi_T)^{-1}\nabla\cdot(\sigma_{eff_T}\nabla u^{(0)}) = \left(r u^{(0)}\left(1-\frac{u^{(0)}}{k}\right)\right), \quad \text{in} \quad \Omega_T\\
&\frac{\partial u^{(0)}}{\partial t} - (\psi_B)^{-1}\nabla\cdot(\sigma_{eff_B}\nabla u^{(0)}) = \left(r u^{(0)}\left(1-\frac{u^{(0)}}{k}\right)\right), \quad \text{in} \quad \Omega_B\\
&u^{(0)}, \sigma\psi_T u_z^{(0)} \qquad \text{continuous} \quad \text{at} \quad \Gamma_T^{'}\\
&u^{(0)}, \sigma\psi_B u_z^{(0)} \qquad \text{continuous} \quad \text{at} \quad \Gamma_B^{'}\\
&u^{(0)} = 0 \quad \text{on} \quad \Gamma_T,\ \Gamma_B
\end{aligned}
$$

where

$$
\begin{aligned}
&\sigma_{eff_T} = \begin{pmatrix} 0 & 0\\ 0 & \sigma\psi_T \end{pmatrix}, \qquad \sigma_{eff_B} = \begin{pmatrix} 0 & 0\\ 0 & \sigma\psi_B \end{pmatrix}\\
&\psi_T = (y_{2_T} - y_{1_T}) = \left(1 - \frac{1}{\pi}\arccos\left(1 + \frac{2D}{A} - \frac{2y}{A}\right)\right)\\
&\psi_B = (y_{2_B} - y_{1_B}) = \left(1 - \frac{1}{\pi}\arccos\left(\frac{2y}{A} + 1\right)\right)
\end{aligned}
$$

Numerical simulations show that, as $\epsilon \to 0$, $u_\epsilon \to u^{(0)}$. The convergence is evaluated in terms of the mean squared error between U and $u^{(0)}$ corresponding to decreasing values of ϵ:

$$
\text{MSE}_\epsilon^t = \frac{1}{N\cdot M}\sum_{i,j=1}^{N,M}(u^{(0)}(x_i,y_j,t) - u_\epsilon(x_i,y_j,t))^2, \quad t = 1\ldots T, \tag{31}
$$

where N and M stand for the number of sampling points in x and y, respectively.

Figure 6 reports the spatial MSE_ϵ^t (31) between homogenized and exact solutions for each time instant and different values of ϵ in semi-logarithmic scale. As we can see, the error decreases as $\epsilon \to 0$.

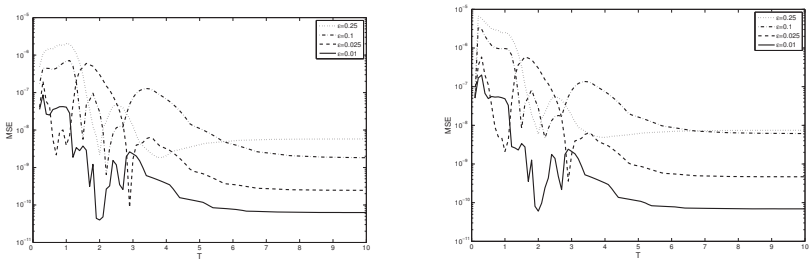

Figure 6. MSE_ϵ^t between the solutions in the interior (left) and near the boundaries (right) of the original (Ω_ϵ) and homogenized (Ω_o) domain (Neumann boundary conditions).

Then, we consider the Dirichlet boundary condition case ($U = 0$) on the rough boundaries Γ_T and Γ_B. Theorem (2) leads to the following equations accounting for the Dirichlet homogenized problem:

$$\begin{aligned}
&\frac{\partial u^{(0)}}{\partial t} - \nabla \cdot (\sigma \nabla u^{(0)}) = r u^{(0)} \left(1 - \tfrac{u^{(0)}}{k}\right), \quad \text{in} \quad \Omega_O \\
&u^{(0)} = 0, \quad \text{in} \quad \Omega_T,\ \Omega_B \\
&u^{(0)} = 0, \quad \text{on} \quad \Gamma_T^{'},\ \Gamma_T,\ \Gamma_B^{'},\ \Gamma_B.
\end{aligned}$$

Numerical simulation show that, as $\epsilon \to 0$, $u_\epsilon \to u^{(0)}$. Figure 7 reports the spatial MSE_ϵ^t (31) between homogenized and exact solutions for each time instant and different values of ϵ in semi-logarithmic scale. As we can see, the error decreases as $\epsilon \to 0$.

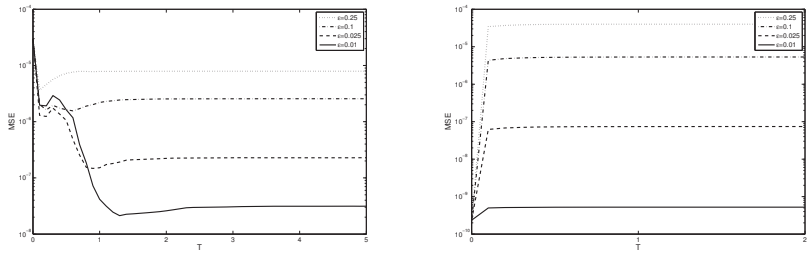

Figure 7. MSE_ϵ^t between the solutions in the interior (left) and near the boundaries (right) of the original (Ω_ϵ) and homogenized (Ω_o) domain (Dirichlet boundary conditions).

Figure 8 reports the comparison of the numerical simulations in the rough and homogenized domains, where Neumann and Dirichlet boundary conditions are assumed in the lower and upper layers of the domain, respectively.

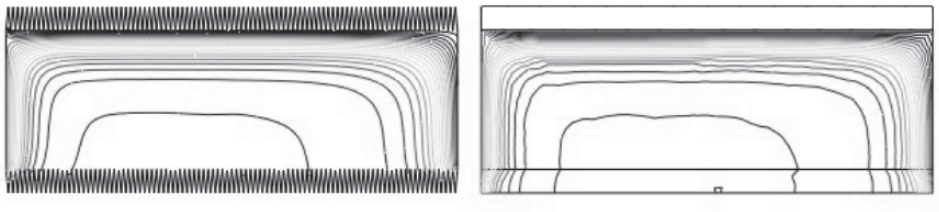

Figure 8. Contour plot of the simulations in the original (left) and homogenized (right) domains for $\epsilon = 0.01$. In the last, we set Neumann boundary conditions in the bottom layer and Dirichlet boundary conditions in the top layer.

Finally, we consider a domain Ω_s whose boundary is decomposed in $\partial\Omega_s = \Gamma_L \cup \Gamma_R \cup \Gamma_{T_s} \cup \Gamma_{B_s}$, where Γ_{T_s} and Γ_{B_s} are two smooth representation of periodic roughness elements Γ_T and Γ_B in the original domain Ω_ϵ. Again, we compare the solutions on the original domain with the one obtained in the smoothed domain Ω_s in terms of the mean squared error defined in (31).
We consider both Neumann and Dirichlet boundary conditions on Γ_{T_s} and Γ_{B_s}. Comparing the numerical simulation we observe that the homogenized model performs considerably better than the smoothed one both with Neumann and Dirichlet boundary conditions (see Figures 9 and 10).

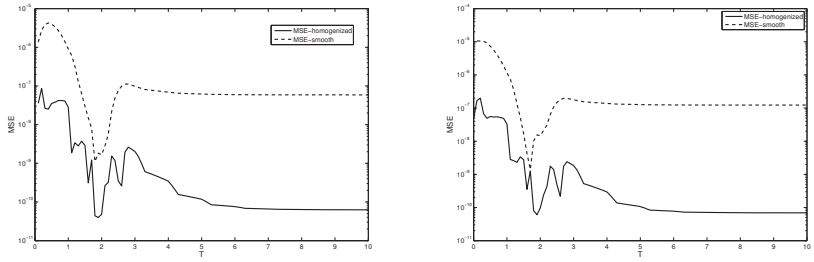

Figure 9. Comparison between MSE_ϵ^t of the homogenized and smoothed solutions for $\epsilon = 0.01$ in the interior (left) and near the boundary (right) of the domain (Neumann boundary conditions).

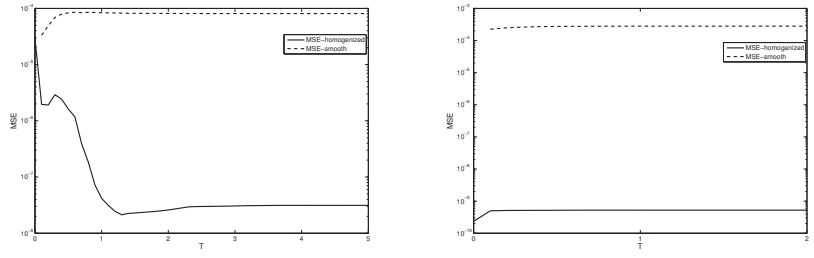

Figure 10. Comparison between MSE_ϵ^t of the homogenized and smoothed solutions for $\epsilon = 0.01$ in the interior (left) and near the boundary (right) of the domain (Dirichlet boundary conditions).

5. APPLICATION TO MULTI-SPECIE ECOLOGICAL MODELS

In this section we apply the above methodology to a class of ecological models for predator-prey interaction of two species in a bounded domain with rough boundary. This is done by extending the previous results obtained for single species to a multi-species context [**42**].

As in Section 4, we consider a rectangular domain Ω_ϵ showing periodic roughness elements Γ_ϵ on the boundaries described by the two curves (28a) and (28b).

We assume that the dynamics of the system is described as follows:

$$\partial_t \mathbf{U} - \mathbf{D}\Delta\mathbf{U} = \mathbf{F}(\mathbf{U}), \quad (x,z) \text{ in } \Omega_\epsilon \ \& \ t \geq 0, \tag{32}$$

where each component of the vector $\mathbf{U} = [U_1(x,z,t), \ldots, U_n(x,z,t)]'$ represents the concentration of each substance (or species), $\mathbf{D} = diag\{\sigma_i\}, i = 1, \ldots, n$ is the matrix of diffusion coefficients, Δ denotes the Laplace operator and

$$\mathbf{F} = [f_1(U_1, \ldots, U_n), \ldots, f_n(U_1, \ldots, U_n)]'$$

accounts for all local reactions. We consider appropriate boundary conditions of either Dirichlet *or* Neumann type. Namely,

$$\text{Dirichlet:} \qquad \mathbf{U} = \mathbf{0} \ , \ (x,z) \text{ on } \Gamma_\epsilon \ , \tag{33}$$

or

$$\text{Neumann:} \qquad \mathbf{DU_n} = \mathbf{0} \ , \ (x,z) \text{ on } \Gamma_\epsilon \ , \tag{34}$$

and suitable smooth initial conditions.

We assume similar hypothesis on existence of solutions independent of ϵ and existence of the Taylor expansions of the functions $f_i(\cdot)$ for $i = 1, \cdots, n$.

Following the procedure described in Section 3, we can summarize the main results in the following remarks.

Remark 1 (Neumann b. c.). Let $\mathbf{U} = [U_1(x,z,t,\epsilon), \ldots, U_n(x,z,t,\epsilon)]'$ satisfy the reaction-diffusion system (32) with Neumann boundary condition (34) on $z = h(y)$ a differentiable 1-periodic function. Suppose that $U_i = u_i(x,y,z,t,\epsilon)$ has the asymptotic form given in equation (9), where u_i is 1-periodic in y. Then, $u_i^{(0)}(x,z,t)$ is independent of y for $-A \leq z \leq 0$ and is a solution of the problem:

$$\begin{array}{l} \partial_t \mathbf{u}^{(0)} - \mathbf{D}\Delta\mathbf{u}^{(0)} = \mathbf{F}(\mathbf{u}^{(0)}), \quad z > 0 \\ \partial_t \mathbf{u}^{(0)} - \mathbf{D_{eff}}\partial_{zz}\mathbf{u}^{(0)} = \mathbf{F}(\mathbf{u}^{(0)}), \quad -A < z < 0 \\ \mathbf{u}^{(0)}, \mathbf{D_{eff}}\partial_z\mathbf{u}^{(0)} \quad \text{continuous at} \quad z = 0 \\ \partial_z \mathbf{u}^{(0)} = 0, \quad z = -A, \end{array} \tag{35}$$

where $\mathbf{u}^{(0)} = [u_1^{(0)}, \ldots, u_n^{(0)}]$, $\mathbf{D} = diag\{\sigma_i\}$, $\mathbf{D_{eff}} = diag\{\sigma_i\, \partial_z(y_2(z) - y_1(z))/(y_2(z) - y_1(z))\}$ and $\mathbf{F}(\mathbf{u}^{(0)}) = [f_1(u_1^{(0)}, \ldots, u_n^{(0)}), \ldots, f_n(u_1^{(0)}, \ldots, u_n^{(0)})]'$.

REMARK 2 (Dirichlet b. c.). Let $\mathbf{U} = [U_1(x, z, t, \epsilon), \ldots, U_n(x, z, t, \epsilon)]'$ satisfy the reaction-diffusion system (32) with Dirichlet boundary condition (33) on $z = h(y)$ a differentiable 1-periodic function. Suppose that $U_i = u_i(x, y, z, t, \epsilon)$ has the asymptotic form given in equation(9), where u_i is 1-periodic in y. Then, $u_i^{(0)}(x, z, t)$ is independent of y for $-A \leq z \leq 0$ and is a solution of the problem:

$$\begin{aligned} &\partial_t \mathbf{u}^{(0)} - \mathbf{D}\Delta\mathbf{u}^{(0)} = \mathbf{F}(\mathbf{u}^{(0)}), \quad z > 0 \\ &\mathbf{u}^{(0)} = 0, \quad -A \leq z \leq 0, \end{aligned} \tag{36}$$

where $\mathbf{u}^{(0)} = [u_1^{(0)}, \ldots, u_n^{(0)}]$, $\mathbf{D} = diag\{\sigma_i\}$ and

$$\mathbf{F}(\mathbf{u}^{(0)}) = [f_1(u_1^{(0)}, \ldots, u_n^{(0)}), \ldots, f_n(u_1^{(0)}, \ldots, u_n^{(0)})]'.$$

The numerical validation of the above results has been performed on the two species predator-prey Rosenzweig-MacArthur model. This model, extensively studied in [**25, 38**], displays a very rich dynamics, including spatial-temporal chaotic behavior and is used to reproduce the dynamics of phytoplankton and zooplankton in aquatic systems. The variable U_1 describes the prey density, whereas U_2 represents the predator density. The interaction between the two species is described by the following equations:

$$\frac{\partial U_1}{\partial t} - \nabla \cdot (\sigma_1 \nabla U_1) = r U_1 \left(1 - \frac{U_1}{k}\right) - q \frac{U_1 U_2}{W + U_1}, \tag{37a}$$

$$\frac{\partial U_2}{\partial t} - \nabla \cdot (\sigma_2 \nabla U_2) = \eta q \frac{U_1 U_2}{W + U_1} - U_2. \tag{37b}$$

As in Section 4, we consider a homogenized domain described by $\Omega_h = \Omega_O \cup \Omega_T \cup \Omega_B$, where the rough boundaries are replaced by two equivalent layers and the coefficients of the homogenized equations are determined by solving the homogenized problem reported in Remarks 1 and 2 for Neumann and Dirichlet boundary conditions, respectively.

The homogenized system equations have the structure reported in equations (35) and (36), where the functions $f_1(u_1^{(0)}, u_2^{(0)})$ and $f_2(u_1^{(0)}, u_2^{(0)})$ are defined according to the RHS of equations (37a) and (37b), respectively. Furthermore, matrices of effective diffusion coefficients $\mathbf{D_{eff_T}}$ and $\mathbf{D_{eff_B}}$, corresponding to the two boundary layers, are the following:

$$\mathbf{D_{eff_T}} = \begin{bmatrix} \sigma_1 \dfrac{\partial_z \psi_T}{\psi_T} & 0 \\ 0 & \sigma_2 \dfrac{\partial_z \psi_T}{\psi_T} \end{bmatrix}, \quad \mathbf{D_{eff_B}} = \begin{bmatrix} \sigma_1 \dfrac{\partial_z \psi_B}{\psi_B} & 0 \\ 0 & \sigma_2 \dfrac{\partial_z \psi_B}{\psi_B} \end{bmatrix},$$

where

$$\begin{aligned} \psi_T = (y_{2_T} - y_{1_T}) &= \left(1 - \frac{1}{\pi} \arccos\left(1 + \frac{2(z-1)}{A}\right)\right), \\ \psi_B = (y_{2_B} - y_{1_B}) &= \left(1 - \frac{1}{\pi} \arccos\left(\frac{2z}{A} + 1\right)\right). \end{aligned} \tag{38}$$

Numerical simulations indicate that, as $\epsilon \to 0$, $\mathbf{U} \to \mathbf{u}^{(0)}$, in terms of the mean squared error defined in (31). Figure 11 reports the spatial MSE between the homogenized and the exact solutions for each time instant and different values of ϵ for Neumann case. As we can see from Figure 12, the error decreases as $\epsilon \to 0$ when the system reaches the steady state.

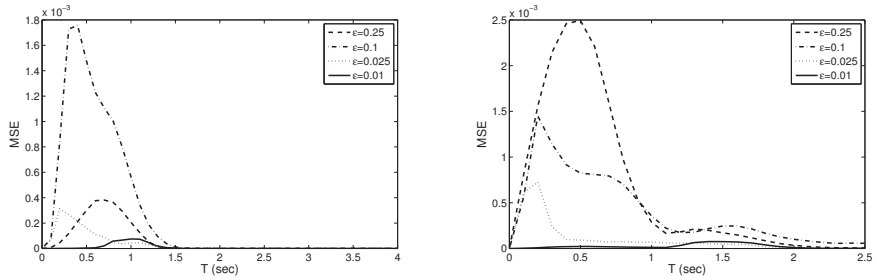

Figure 11. MSE between original and homogenized solutions U_1 (left) and U_2 (right) for Neumann boundary conditions.

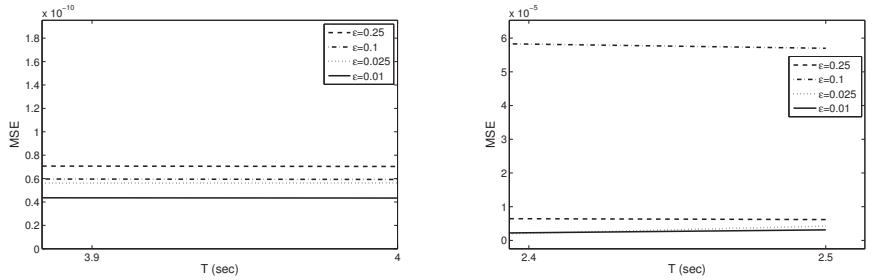

Figure 12. Steady state MSE between original and homogenized solutions U_1 (left) and U_2 (right) for Neumann boundary conditions.

6. ROUGHNESS INDUCED SPATIO-TEMPORAL SHIFTS IN THE DYNAMICS

In this section we address the problem of evaluating the effects induced by the presence of rough boundaries in the spatio-temporal dynamics of systems described by reaction-diffusion partial differential equations. To this purpose, we compare the solution of a system showing complex patterns in a homogenized rough boundary domain and in a regular square domain. We emphasize that use of the homogenized version of the systems was crucial in computing the different recurrence indicators accurately in a feasible time.

Theorem 1 stated that the diffusion coefficient in the homogenized equations is an effective one and, under Neumann boundary conditions, depends on the spatial variable y: $\langle\sigma\rangle = \sigma(y_2 - y_1)$ showing that the roughness of the boundary is accounted by the spatial dependence of the diffusion parameter. Non constant

diffusion coefficients may in general induce changes in the dynamical features of the systems under consideration [**35**]. If the model is nonlinear, such changes may also generate complex patterns. In particular, in [**13**] differences in the spatial organization of the Turing instabilities are reported for the asymptotic solutions of reaction-diffusion equations.
In order to verify the presence of such behaviors in the homogenized equations, we consider a prototypical reaction diffusion system showing complex patterns. The model describes a series of hypothetical trimolecular auto-catalytic reactions proposed by Schnakenberg [**51**]. The dimensionless version takes the form [**43**]:

$$\begin{aligned} u_t - \nabla \cdot (\nabla u) &= \gamma(a - u + u^2 v) = \gamma f(u,v), \\ v_t - \nabla \cdot (d \nabla v) &= \gamma(b - u^2 v) = \gamma g(u,v), \end{aligned} \tag{39}$$

where L is the typical length scale and

$$u = A\left(\frac{k_3}{k_2}\right)^{1/2},\ v = B\left(\frac{k_3}{k_2}\right)^{1/2},\ t = \frac{D_A t}{L^2},\ \mathbf{x} = \frac{\mathbf{x}}{L},$$
$$d = \frac{D_B}{D_A},\ a = \frac{k_1}{k_2}\left(\frac{k_3}{k_2}\right)^{1/2},\ b = \frac{k_4}{k_2}\left(\frac{k_3}{k_2}\right)^{1/2},\ \gamma = \frac{L^2 k_2}{D_A}.$$

The critical diffusion coefficient d_c, giving rise to Turing instabilities and critical wavenumber k_c^2, are obtained by linearization near the steady state $(u_0, v_0) = \left((b+a), \frac{b}{(b+a)^2}\right)$ as follows:

$$d_c = \frac{(b+a)\left[(b+a)(3b+a) + 2(2b(b+a)^3)^{1/2}\right]}{(b-a)} \tag{40}$$

$$k_c^2 = \gamma\left(\frac{(b^2-a^2)}{(3b^2+4ab+a^2+2(2b(b+a)^3)^{1/2})}\right)^{1/2}. \tag{41}$$

Assuming that the system is solved in a rough domain, the solutions of the system are homogenized using multiple-scale analysis following the methodology described in the previous sections. As before, the original rough boundary domain Ω_ϵ, bounded above and below by equations (28a) and (28b), is replaced by a homogenized one $\Omega_h = \Omega_O \cup \Omega_T \cup \Omega_B$. For such homogenized system the following equations hold:

$$\begin{aligned} &\partial_t \mathbf{u}^{(0)} - \mathbf{D}\Delta \mathbf{u}^{(0)} = \mathbf{F}(\mathbf{u}^{(0)}), \quad \text{in} \quad \Omega_O \\ &\partial_t \mathbf{u}^{(0)} - \mathbf{D_{eff_T}} \partial_{zz} \mathbf{u}^{(0)} = \mathbf{F}(\mathbf{u}^{(0)}), \quad \text{in} \quad \Omega_T \\ &\partial_t \mathbf{u}^{(0)} - \mathbf{D_{eff_B}} \partial_{zz} \mathbf{u}^{(0)} = \mathbf{F}(\mathbf{u}^{(0)}), \quad \text{in} \quad \Omega_B \\ &\mathbf{u}^{(0)}, \mathbf{D_{eff_T}} \partial_z \mathbf{u}^{(0)} \quad \text{continuous at} \quad \Gamma_T^{'} \\ &\mathbf{u}^{(0)}, \mathbf{D_{eff_B}} \partial_z \mathbf{u}^{(0)} \quad \text{continuous at} \quad \Gamma_B^{'} \\ &\partial_z \mathbf{u}^{(0)} = 0, \quad \text{on} \quad \Gamma_T,\ \Gamma_B, \end{aligned} \tag{42}$$

where

$$\mathbf{u}^{(0)} = \begin{bmatrix} u^{(0)} \\ v^{(0)} \end{bmatrix}, \quad \mathbf{F}(\mathbf{u}^{(0)}) = \begin{bmatrix} \gamma f(u^{(0)}, v^{(0)}) \\ \gamma g(u^{(0)}, v^{(0)}) \end{bmatrix} = \begin{bmatrix} \gamma(a - u^{(0)} + {u^{(0)}}^2 v^{(0)}) \\ \gamma(b - {u^{(0)}}^2 v^{(0)}) \end{bmatrix},$$

$$\mathbf{D} = \begin{bmatrix} 1 & 0 \\ 0 & d \end{bmatrix}, \quad \mathbf{D_{eff_T}} = \begin{bmatrix} 1 & 0 \\ 0 & d\dfrac{\partial_z \psi_T}{\psi_T} \end{bmatrix}, \quad \mathbf{D_{eff_B}} = \begin{bmatrix} 1 & 0 \\ 0 & d\dfrac{\partial_z \psi_B}{\psi_B} \end{bmatrix},$$

$$\psi_T = (y_{2_T} - y_{1_T}) = \left(1 - \frac{1}{\pi}\arccos\left(1 + \frac{2(z-1)}{A}\right)\right)$$

$$\psi_B = (y_{2_B} - y_{1_B}) = \left(1 - \frac{1}{\pi}\arccos\left(\frac{2z}{A} + 1\right)\right).$$

In order to observe the effect of rough boundaries in the system solutions, we have designed a series of systematic experiments by varying the diffusion coefficient.

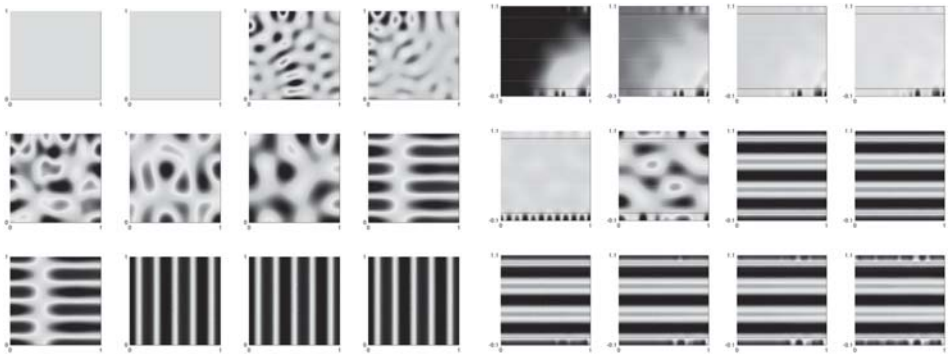

Figure 13. Spatial pattern for $\gamma = 800$, $a = 0.1$ and $d = \{9.5, 9.6, \ldots, 10.6\}$. Left: Solutions on the regular domain. Right: Solutions on the homogenized domain.

Figure 13 shows the approximate solutions of the system for the regular (left) and the homogenized (right) domain. Each inset corresponds to a steady state solution that has been obtained by fixing the parameters a, b and γ and varying the diffusion coefficient d in an interval including the critical value d_c for which the Turing instability occurs as in equations (40) and (41).

One can observe the differences between the solutions in the regular and in the homogenized domains accounting for a highly oscillating boundary. Figure 13, where $a = 0.1$, shows two main differences: the first difference concerns the formation of patterns with different structures. The presence of different patterns in the same system is reported in [**34**] and explained by means of numerical implications involving the size of the spatial domain of integration and typical shapes depending on the model equations. The second and more important difference is related to the values of the diffusion parameter for which the formed pattern is stable. As one can see, the stable Turing patterns are reached after a spatial transient, during which partially formed structures are observed. These stable patterns are obtained

at lower values of d in the case of homogenized system with respect to the regular ones, anticipating the bifurcations. This fact can be explained by the dependence of the diffusion coefficient on the spatial variable z, as shown at the beginning of this section.

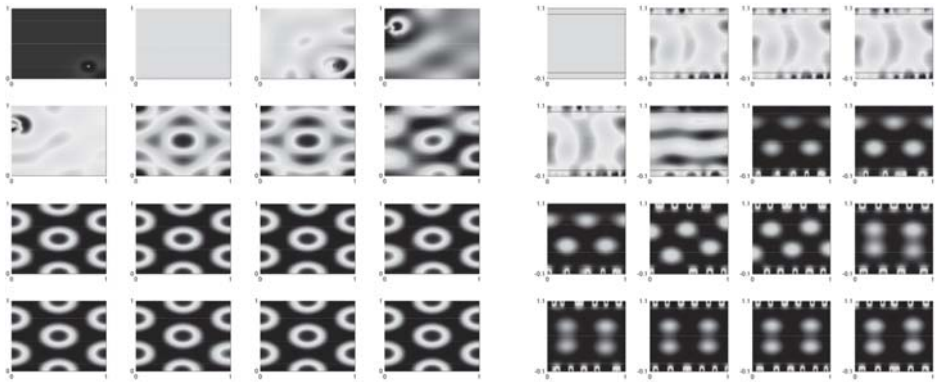

Figure 14. Spatial pattern for $\gamma = 800$, $a = 0.3$ and $d = \{28, 28.2, \ldots, 31\}$. Left: Solutions on the regular domain. Right: Solutions on the homogenized domain.

If we focus on Figure 14, the same mechanism is not observed: in this case the value of the parameter $a = 0.3$ is such that the critical diffusion parameter d_c is higher, thus inducing a faster diffusion process in both the smooth and rough systems. In [**13**] the possibility of having sequences of bifurcations, e.g., two Turing bifurcations, leading to changes in the spatial pattern structure is discussed. A similar phenomenon is observed in the simulations on the left part of Figure 14, where the homogenized solution of the SCHNAKENBERG system (42) is shown: the Turing structure is slightly modified by increasing the diffusion coefficient, while the same phenomenon is not present in the solutions of the smoothed boundary system (see the left part of the Figure 14).

6.1. Spatial recurrence indicators

In order to quantify the changes in the dynamics induced by rough boundaries, we use a recurrence index, namely the determinism, introduced in the field of nonlinear time series analysis and recently extended to the spatial case in [**39, 40**]. In this case the determinism is used for measuring the differences between the model simulations in regular and homogenized domains.

In the sequence, we present a short description of the recurrence methods for spatial systems. For a deeper treatment of the methodology applied to the time series and to d-dimensional spatial systems, the reader is referred to [**37**] and [**36**], respectively. For the purposes of the present work, we only define the recurrence indicators for spatially distributed systems and we apply them to the 2-dimensional spatial case of the Schnackenberg system.

In [**36**] the Generalized Recurrence Plot (GRP) has been introduced for a d-dimensional data-set, where the $2d$-dimensional RP is specified by the matrix $\mathbf{R}$,

whose elements are:

$$\mathbf{r}_{\vec{i},\vec{j}} = \Theta(\xi - ||\vec{x}_{\vec{i}} - \vec{x}_{\vec{j}}||), \tag{43}$$

where $\vec{i} = i_1, i_2, \ldots, i_d$ is the d-dimensional coordinate vector and $\vec{x}_{\vec{i}}$ is the associated phase-space vector, $\Theta(\cdot)$ is the unit step function, ξ is the tolerance level, and $||\cdot||$ is a chosen norm (typically the Euclidean one). In the graphical representation, each non-zero entry of the RP matrix $\mathbf{R}$ is marked by a black dot in the position $(\vec{i}, \vec{j})$. This GRP accounts for the recurrences between the d-dimensional state vectors. Since any point is recurrent with itself, a linear manifold of dimension d exists in the RP, for which $\mathbf{r}_{\vec{i},\vec{j}} = 1$, $\forall \vec{i} = \vec{j}$. Although the RP cannot be visualized easily, its quantification by means of suitable indicators has been made possible by the Generalized Recurrence Quantification Analysis (GRQA) [**36**].

More recently, the application of GRP and GRQA analysis to the study of two dimensional spatio-temporal systems and complex images, consisting in the fixed time solutions of 2-dimensional distributed systems, has been proposed [**39, 40**].

From the mathematical point of view, an image is a two-dimensional Cartesian object composed of scalar values and in this special case the elements of the matrix $\mathbf{R}$ in the GRP are:

$$\mathbf{r}_{i_1,i_2,j_1,j_2} = \Theta(\xi - |x_{i_1,i_2} - x_{j_1,j_2}|) \quad i_1, i_2, j_1, j_2 = 1, \ldots, N, \tag{44}$$

where each black dot represents a spatial recurrence between two pixels, and every pixel is identified by its coordinates (i_1, i_2), being i_1 and i_2 the row and the column index respectively. In this case, the recurrence plot is a four-dimensional RP and contains the two-dimensional identity plane, denoted LOI in analogy with the "Line of Identity" in the one dimensional case, defined by setting $i_1 = j_1$ and $i_2 = j_2$.

As mentioned above, due to their dimension and to the limited screen resolution it is difficult to analyze the RP only by means of visual inspection. To cope with this problem, the RQA offers a set of indicators computed on the structures of the RP, from which we mention the Recurrence Rate (RR) and the Determinism (D).

In the RPs recurrent points may form structures parallel to the LOI, such as lines in one dimensional time series and planes in two dimensional spatial time series. Denoting by ℓ the length of a line structure, for example defined by a sequence of ℓ black dots belonging to the diagonal of each recurrent subset of the RP, we build the histogram $P(\ell)$ of the line lengths and define the GRQA measures on the basis of their distribution. In particular, RR and D are defined as follows:

$$RR = \frac{1}{N^4} \sum_{i_1,i_2,j_1,j_2}^{N} \mathbf{r}_{i_1,i_2,j_1,j_2} = \frac{1}{N^4} \sum_{\ell=1}^{N} \ell P(\ell), \quad D = \frac{\sum_{\ell=\ell_{\min}}^{N} \ell P(\ell)}{\sum_{\ell=1}^{N} \ell P(\ell)}, \tag{45}$$

where ℓ_{min} is the minimum length considered for the diagonal structures.

The recurrence measures are related to the physical properties of the image under consideration, since they account for recurrent properties of the structures visible in the image itself and consequently define a sort of spatial correlation. In particular, the RR is the fraction of recurrent points with respect to the total number of possible recurrences and D is the fraction of recurrent points forming diagonal structures with respect to all the recurrences. Then, RR is a density measure of the RP, while D has been introduced as a measure of the predictability of the system, because it accounts for the diagonal structures in the RP. For example, the presence of such structures in the RP is related to periodicities in the structure of the image.

The above techniques are applied to the solutions, taken at fixed time instants, of the two dimensional spatial Schanckenberg system, described by equation (39) and simulated in a regular domain and for its homogenized version, described by System (42). The corresponding numerical simulations account for the presence of a rough domain. In particular, the determinism is applied to the insets of Figures 13 and 14, according to the experiments set up at the beginning of the section.

Figure 15 reports the determinism for different values of the diffusion parameter d, $a = 0.1$ and different boundaries. As one can notice, the indicator decreases for values of d corresponding to the critical value d_c for which the Turing bifurcation occurs. Furthermore, in the homogenized model the decreasing is anticipated ($d = 10.1$) with respect to the regular one ($d = 10.4$).

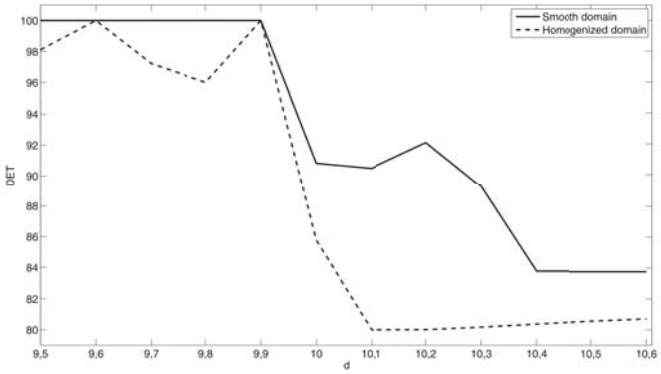

Figure 15. Determinism for $a = 0.1$ in the regular and homogenized domains.

This fact is confirmed by observing Figure 13, where the stable pattern is formed at values $d = 10.4$ and $d = 10.1$ in the regular and homogenized solutions, respectively.

Similar results hold for $a = 0.3$, where a 10% reduction of determinism is observed at the critical values of the diffusion coefficient d (see Figure 16). The anticipation in the stabilization of the spatial pattern is not precisely detected because of the high sensitivity of the dynamics with respect to the diffusion parameter.

We emphasize that use of the homogenized version of the systems was crucial in computing the different recurrence indicators accurately in a feasible time.

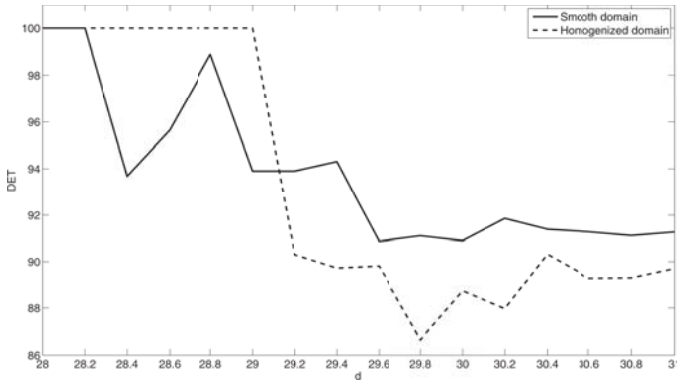

Figure 16. Determinism for $a = 0.3$ in the regular and homogenized domains.

7. CONCLUSIONS

In this paper, the homogenization of nonlinear reaction-diffusion equations of distributed systems in domains with rough boundaries is proposed. The main novelty of the work is the use of a multiple-scale approach to reduce the complexity of the geometry of the boundary for reaction-diffusion systems. In this context, formal homogenization theorems have been proved, allowing one to replace the roughness of the boundary with an equivalent layer where suitable modified equations hold. In the solution of the homogenized equation the influence of the roughness is accounted for by means of some "effective" parameters. Both Neumann and Dirichlet boundary conditions are taken into account. Using the discretization in the finite element method of lines, numerical simulations have been performed to test the convergence of the solutions. A comparison with the solution in a smoothed domain is also presented.

The possibility of parametrizing the boundary data by means of effective boundary conditions increases the robustness and stability of the numerical solution methods that handle the reaction-diffusion problems under consideration. This in turn, would be instrumental in the development of good identification techniques of the relevant parameters for the model from measured data. Indeed, one of the sources of instability in the ill-posed inverse problem of identifying model parameters, such as the diffusion coefficient σ or the function f in equation (1), is associated to the difficulty in describing the complex boundary conditions and keeping track of their effect. Finding an effective description of the asymptotic behavior of the solutions may help in removing a crucial source of instability.

Moreover, the paper presents the application of the homogenization theorem to extended predator-prey ecological models.

The analysis of changes in the dynamics of systems showing complex patterns, such as the Schnackenberg system, is also presented. The results of the study show that the systems solved in regular and homogenized domain present switches in the

dynamics in the sense that, for example, structural stability breaking may arise at different values of the diffusion coefficients. In the presented application, the homogenized Schnackenberg system "anticipates" the Turing bifurcation reaching a steady spatial state faster than the system solved in regular boundaries.

A further development of the present work would be to consider mixed boundary conditions of Robin type. The latter seem to be very common in situations where the boundary is neither completely reflecting nor completely absorbing. In this case, the possibility of describing effectively such boundary would once again help in identification problems. The implications of the present work for the solution of model identification problems of distributed systems are currently under investigation by the authors.

The generality of the system we are considering does not allow rigorous convergence results without imposing a number of additional hypothesis that would lead us too far out of the scope of this work. Indeed, it is well-know that even simple reaction-diffusion equations with nontrivial reaction terms may lead to blow-ups or solution break-downs. The same remark holds for the degenerate parabolic system obtained for the homogenized solution in Equations (10a) and (10b). Here again, the availability of rigourous existence and uniqueness results depends on additional hypothesis on the function $f(u)$. Indeed, there is an extensive literature on the subject of degenerate parabolic equation. See for example [**28, 22, 23, 48**]. The situation is further complicated by the coupling through the boundary $z = 0$ between the solutions of Equations (10a) and (10b).

As in Nevard and Keller [**45**], the present work did not consider the well-posedness of the problem and focused only on the formal part of the theory of the asymptotics. A natural theoretical follow up of this work would be to consider the well-posedness of Equations (10a) and (10b).

Acknowledgments. JPZ was supported by CNPq under grants 302161/2003-1 and 474085/2003-1. JPZ acknowledges the hospitality of the Università di Siena, where most this research was carried through. CM and ES thank Instituto Nacional de Matemática Pura e Aplicada for the invitations to numerous and stimulating events on biomathematics.
The authors heartily thank Angelo Facchini and Antonio Vicino for their invaluable help and support throughout the research.

REFERENCES

1. Y. Achdou, P. Le Tallec, F. Valentin, O. Pironneau: *Constructing wall laws with domain decomposition or asymptotic expansion techniques.* Comput. Methods Appl. Mech. Engrg., **151** (1998), 215–232. Symposium on Advances in Computational Mechanics, Vol. **3** (Austin, TX, 1997).

2. Y. Achdou, B. Mohammadi, O. Pironneau, F. Valentin: *Domain decomposition and wall laws.* Sūrikaisekikenkyūsho Kōkyūroku, **989** (1997), 42–55. Domain decomposition methods and related topics (Kyoto, 1996).

3. Y. Achdou, O. Pironneau: *Domain decomposition and wall laws.* C. R. Acad. Sci. Paris Sér. I Math., **320** (1995), 541–547.

4. Y. Achdou, O. Pironneau, F. Valentin: *Effective boundary conditions for laminar flows over periodic rough boundaries.* J. Comput. Phys., **147** (1998), 187–218.

5. Y. Amirat, O. Bodart, U. De Maio, A. Gaudiello: *Asymptotic approximation of the solution of the Laplace equation in a domain with highly oscillating boundary.* SIAM J. Math. Anal., **35** (2004), 1598–1616 (electronic).

6. Y. Amirat, O. Bodart, U. De Maio, A. Gaudiello: *Asymptotic approximation of the solution of Stokes equations in a domain with highly oscillating boundary*, Ann. Univ. Ferrara Sez. VII Sci. Mat., **53** (2007), 135–148.

7. Y. Amirat, O. Bodart, U. De Maio, A. Gaudiello: *Effective boundary condition for Stokes flow over a very rough surface*, J. Differential Equations, **254** (2013), 3395–3430.

8. J. M. Arrieta, A. N. Carvalho, M. C. Pereira, R. P. Silva: *Semilinear parabolic problems in thin domains with a highly oscillatory boundary.* Nonlinear Anal., **74** (2011), 5111–5132.

9. J. M. Arrieta, M. C. Pereira: *Elliptic problems in thin domains with highly oscillating boundaries.* Bol. Soc. Esp. Mat. Apl. SeMA, **51** (1) (2010), 17–24.

10. J. M. Arrieta, M. C. Pereira: *Homogenization in a thin domain with an oscillatory boundary.* J. Math. Pures Appl. (9), **96** (1) (2011), 29–57.

11. J. M. Arrieta, M. C. Pereira: *The Neumann problem in thin domains with very highly oscillatory boundaries.* J. Math. Anal. Appl., **404** (2013), 86–104.

12. A. Assireu, F. Roland, E. Novo, N. O. Barros, J. L. Stech, F. S. Pacheco: *Existe relação entre a complexidade geomátrica do entorno dos reservatórios e a variabilidade espacial dos parametros limnológicos?.* 2007. Anais XIII Simpósio Brasileiro de Sensoriamento Remoto, 21–26 April 2007, Florianópolis, Brasil.

13. D. Benson, P. Maini, J. Sherratt: *Analysis of pattern formation in reaction diffusion models with spatially inhomogenous diffusion coefficients.* Math. Comput. modelling, **17** (1993), 29–34.

14. L. M. Bini, J. G. Tundisi, T. Matsumura-Tundisi, C. E. Matheus: *Spatial variation of zooplankton groups in a tropical reservoir (Broa Reservoir, São Paulo State-Brazil).* Hydrobiologia, **357** (1997), 89–98.

15. A. Bradji, E. Holzbecher: *On the Convergence Order of COMSOL Solutions.* Proc. of the COMSOL Users Conference, Grenoble, 2007.

16. A. Bradji, E. Holzbecher: *On the Convergence Order in Sobolev Norms of COMSOL Solutions.* Proc. of the COMSOL Conference, Budapest, 2008.

17. R. Brizzi: *Transmission problem and boundary homogenization.* Rev. Mat. Apl., **15** (1994), 1–16.

18. R. Brizzi, J. P. Chalot: *Homogénéisation de frontiére.* Ph.D Thesis, Dep. of Mathematics, Université de Nice. Nice. France, 1978.

19. A. C. Carius, A. L. Madureira: *Hierarchical modeling of the heat equation in a heterogeneous plate.* Appl. Numer. Math., **59** (2009), 2105–2118.

20. G. A. Chechkin, A. L. Piatnitski, A. S. Shamaev. *Homogenization.* vol. **234** of Translations of Mathematical Monographs, American Mathematical Society, Providence, RI, 2007. Methods and applications, Translated from the 2007 Russian original by Tamara Rozhkovskaya.

21. D. Cioranescu, P. Donato: *An introduction to homogenization.* vol. **17** of Oxford Lecture Series in Mathematics and its Applications, The Clarendon Press Oxford University Press, New York, 1999.

22. P. D'Ancona, S. Spagnolo: *The Cauchy problem for weakly parabolic systems.* Math. Ann., **309** (1997), 307–330.

23. E. DiBenedetto: *Degenerate parabolic equations.* Universitext. New York, NY: Springer-Verlag. xv, 387p. DM 88.00/pbk , 1993.

24. J. Garnier, R. Kraenkel, A. Nachbin: *Optimal Boussinesq model for shallow-water waves interacting with a microstructure*. Physical Review E, **76** (2007), p. 046311.

25. M. R. Garvie: *Finite-Difference Schemes for Reaction-Diffusion Equations Modeling Predator-Prey Interactions in MATLAB*. Bull. Math. Biol., **69** (2007), 931–956.

26. P. Grindrod: *The theory and applications of reaction-diffusion equations*: *Patterns and waves.* 2*nd ed.* Oxford Applied Mathematics and Computing Science Series. Oxford: Clarendon Press., 1996.

27. T. Hughes: *The finite element method: linear static and dynamic finite element analysis.* Prentice-Hall Englewood Cliffs, NJ., 1987.

28. K. Igari: *Degenerate parabolic differential equations*, Publ. Res. Inst. Math. Sci., **9** (1973/74), 493–504.

29. J. Keller, D. W. McLaughlin, G. C. Papanicolaou: *Surveys in Applied Mathematics.* Plenum Press, 1995.

30. W. Kohler, G. Papanicolaou, S. Varadhan: *Boundary and interface problems in regions with very rough boundaries.* Multiple scattering and waves in random media, Proc. Workshop, Blacksburg/Va. 1980, 165–197, 1981.

31. S. MacIntyre, J. R. Romero, G. W. King: *Spatial-temporal variability in surface layer deepening and lateral advection in an embayment of Lake Victoria*, Limnol. Oceanogr., **43** (2002), 656–671.

32. A. Madureira, F. Valentin, *Analysis of curvature influence on effective boundary conditions.* C. R. Math. Acad. Sci. Paris, **335** (2002), 499–504.

33. A. L. Madureira: *A multiscale finite element method for partial differential equations posed in domains with rough boundaries*, Math. Comp., **78** (2009), 25–34.

34. A. Madzvamuse, P. K. Maini, A. J. Wathen: *A moving grid finite element method for the simulation of pattern generation by turing models on growing domains*, 2004.

35. P. Maini, D. Benson, J. Sherratt: *Pattern formation in reaction-diffusion models with spatially inhomogeneous diffusion coefficients.* Math. Med. Biol., **9** (1992), 197–213.

36. N. Marwan, J. Kurths, P. Saparin: *Generalised recurrence plots analysis for spatial data.*, Phys. Lett. A, **360** (2007), 545–551.

37. N. Marwan, M. C. Romano, M. Thiel, J. Kurths: *Recurrence plots for the analysis of complex systems.*, Phys. Reports, **438** (2007), 237–329.

38. A. B. Medvinsky, S. V. Petrovskii, I. A. Tikhonova, H. Malchow, B. L. Li: *Spatiotemporal complexity of plankton and fish dynamics.* SIAM review, **44** (2002), 311–370.

39. C. Mocenni, A. Facchini, A. Vicino: *Identifying the dynamics of complex spatio-temporal systems by spatial recurrence properties.* PNAS, **107** (2010), 8097–8102.

40. C. Mocenni, A. Facchini, A. Vicino: *Comparison of recurrence quantification methods for the analysis of temporal and spatial chaos.* Math. Comput. Modelling, **53** (2011), 1535–1545.

41. C. Mocenni, E. Sparacino, A. Vicino, J. P. Zubelli: *Mathematical modelling and parameter estimation of the Serra da Mesa basin.* Math. Comput. Modelling, **47** (2008), 765–780.

42. C. Mocenni, E. Sparacino, J. P. Zubelli: *Homogenization of Multi-Spieces Reaction-Diffusion Systems in Domains with Rough Boundaries.* In: AIP Conference Proceedings, vol. **1168**, 2009, p. 89.

43. J. Murray: *Mathematical biology. Vol.* 2 : *Spatial models and biomedical applications.* 3*rd revised ed.* Interdisciplinary Applied Mathematics. 18. New York, NY: Springer. xxv, 811 p., 2003.

44. A. Nachbin, W. Choi: *Nonlinear waves over highly variable topography.* Eur. Phys. J. Special Topics, **147** (2007), 113–132.

45. J. Nevard, J. B. Keller: *Homogenization of rough boundaries and interfaces.* SIAM J. Appl. Math., **57** (1997), 1660–1686.

46. J. Nolen, G. Papanicolaou, O. Pironneau: *A framework for adaptive multiscale methods for elliptic problems.* Multiscale Model. Simul., **7** (2008), 171–196.

47. M. C. Pereira, R. P. Silva: *Error estimates for a Neumann problem in highly oscillating thin domains.* Discrete Contin. Dyn. Syst., **33** (2013), 803–817.

48. F. Punzo: *Uniqueness of solutions to degenerate parabolic and elliptic equations in weighted Lebesgue spaces.* Math. Nachr., **286** (2013), 1043–1054.

49. J. Ripa, A. Ives: *Food web dynamics in correlated and autocorrelated environments.* Theoretical Population Biology, **64** (2003), 369–384.

50. A. B. Ryabov, B. Blasius: *Population growth and persistence in a heterogeneous environment*: *The role of diffusion and advection* Math. Model. Nat. Phenom., **3** (2008), 42–86.

51. J. Schnackenberg: *Simple chemical reaction systems with limit cycle behaviour.* J. Theor. Biol., **81** (1979), 389–400.

Dipartimento di Ingegneria
dell'Informazione e Scienze Matematiche,
Univ. di Siena,
via Roma, 56, 53100 Siena
Italy
E-mails: mocenni@dii.unisi.it
emiliano.s@gmail.com

Instituto Nacional de Matemática Pura e Aplicada,
Estrada Dona Castorina 110,
22460-320, Rio de Janeiro
Brazil
E-mail: zubelli@impa.br

(Received August 18, 2013)
(Revised January 16, 2014)